Energy absorption capacity of braided frames under bending loads

R. Sturm *) 1) • F. Heieck 2)

1) *Institute of Structures and Design, German Aerospace Center (DLR), Germany*

2) *Institute of Aircraft Design, University of Stuttgart, Germany*

Abstract

The energy absorption capacity of braided composite frames under bending loads was studied by conducting quasi-static four-point-bending tests. As specimen geometry C-shaped frame segments where chosen which show the typical failure behaviour of frames with open cross section, such as local buckling and crippling. The braiding manufacturing process offers the possibility to influence the fracture mechanics by a local hybridization of the braider yarns. Different hybridization concepts were investigated to identify design principles for braided frame structures with enhanced energy absorption capacity. The test results show that the post-failure energy absorption of braided frame segments can be significantly increased by a local modification of the braid architecture.

1. Introduction

Whilst braided composites are already used in many applications such as fan blade containment or as energy-absorbing crash structures in racing cars there is interest to increase the usage of braided composites for further structural components in the aerospace and automotive fields. The main reason for the growing interest is the requirement of the industries for cost-efficient highly automated manufacturing of high performance composite structures. Braids are often manufactured using rotary braiding machines which can be tailored to provide a wide variety of complex preform shapes. In comparison to non-crimped fabrics, 2D-braids feature a high impact resistance and crash energy absorption potential, while still remaining competitive regarding stiffness and strength properties. In the braiding process closed, tubular shaped structures can be produced, which are particularly suitable for manufacturing of frames, crash elements and other structural beam components. The tow waviness of braids acts as reinforcement through thickness which provides an improved damage tolerance for braided structures.
The understanding of the mechanical properties and the failure mechanisms of braids is important for the design process of braided structures. In the literature studies can be found which investigate the mechanical performance of 2-D braided carbon/epoxy composites in comparison to laminates made of unidirectional tape. Due to twisting and fibre misalignment of fibre tows braided composites show a 10 % reduced stiffness in tension and compression [1]. Due to the fibre damage during the braiding process and due to the undulation of the braid fibre path the failure strength values are 20 % - 30 % lower compared to unidirectional tape specimens [1,2]. Swanson and Smith investigated the strength properties of triaxial braided composites under biaxial loading conditions. The experimental study showed similar shaped failure envelopes for triaxial braid and laminates under biaxial loading. The biaxial failure properties of triaxial braid can be obtained by using critical strain values in the axial and braid direction, but with degraded strength properties due to the undulating nature of the fibre path [2,3]. Potluri et al. [4] investigated the flexural and torsional behaviour of

biaxial and triaxial braided composite structures. For the assessment of the flexural behaviour, 3-point bending test on turbular specimens were conducted to investigate the influence of the braiding angle on bending stiffness. Experimental studies investigating the strain rate dependency of 2D biaxially and triaxially reinforced braided composites found strain rate dependent behaviour for stiffness, strength and onset of damage [5]. In the literature numerous publications can be found investigating the numerical assessment of the material characteristics of braided composites on mesoscale level [6 - 9]. Due to the necessary detailed discretisation of fibre tows and resin, this approach is not applicable on the structural level. Limited studies can be found in the literature addressing modelling strategies for components made out of braided composite material [10].
The specific energy absorption of composite structures which are designed to absorb kinetic energy by crushing is significantly higher compared to those which are designed to absorb kinetic energy by bending. This is a significant disadvantage for the application of composite materials for crash related structural components since metals can absorb energy by plastification independent of the failure mode. In the field of aerospace the importance of frames with increased energy absorption capacity after bending failure was identified for composite fuselage sections, if the vertical acceleration loads of the passengers should not exceed values typical for a metallic fuselage design [11,12]. Limited experimental studies are published, investigating the energy absorption characteristics of composite frame structures under bending loads. In [13] damage initiation and energy absorption of twin-walled fuselage panels with foldcore were investigated. The study showed that position and failure load can be adapted according to the defined kinematic hinge requirements by adjusting locally the through-thickness compression strength of the core. Bending failure of CFRP frame segments with epoxy resin were studied by Pérez [14] and Heimbs [15]. The improvement of the energy absorption capacity of CFRP frames was investigated for frame segments made out of AS4/PEEK [11] [16]. In this study ductile titanium sheets were embedded in the flange laminate of C-shaped frame segments. In the experiments the hybridisation did not provide significant improvement in the energy absorption capacity after bending failure compared to frame segments purely made out of CFRP.
Since braided composites are commonly recognized as a promising concept for future frame design, the presented study contributes to the development of design principles for fibre architecture and hybridisation of braided frames with enhanced energy absorption capacity under bending loads.

2. Specimen Definition and Manufacturing

The energy absorption capacity of braided composites was studied by conducting quasi-static four-point-bending tests. Generic C-shaped frame segments were chosen as specimen geometry, since this geometry shows the typical bending failure characteristics of open frame profiles. Frames with an open cross section typically fail due to instability failure of the compressed frame flange (crippling). Figure 1 shows the test setup and the specimen definitions. The specimen was encased in aluminium fittings in the region of load introduction to avoid failure initiation in the area of stamp and support. Additionally the solid fittings stabilize the test specimen against lateral displacement due to bending-torsion coupling effects. In the final test setup the distance between the two supports was L_{su} = 640 mm, the distance between the stamps had a distance of $L_{\Delta s}$ = 300 mm and the free length of the test specimen was L_C = 260 mm.
Figure 1 depicts additionally the dimensions of the C-shaped test specimen. The cross-sectional dimensions of the test specimens were H = 80 mm for the web height and B = 38 mm for flange width. The radius between flange and web was R = 4 mm. The test specimens had a length of 600 mm. For the applied modification of the fibre architecture the flange was defined to include the complete radius area between web and flange.

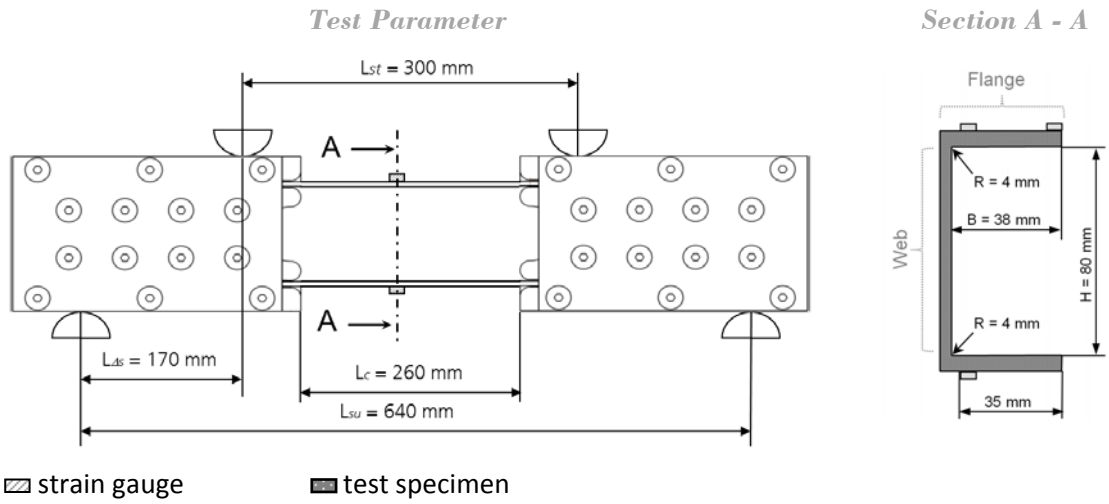

Fig. 1: Schematic drawing of the four-point-bending test and parameters of the test specimen

For compensation of the variable laminate thicknesses the test specimens were embedded into the aluminium fittings using epoxy resin as filling material between test specimen and fixture. The aluminium fittings were treated with release agent to allow the dis-assembly of the aluminium fittings and the test specimen. Therefore, the boundary conditions of the load introduction correspond to a loose clamping of the test specimen within the casing. Three strain gauges were used to measure local strains in the centre section of the test specimen.

For manufacturing of the braided test specimens a quadrangular shaped mandrel made out of aluminium was used. The mandrel design enabled a direct infiltration after the braiding process using the Vacuum Assisted Resin Injection (VARI) process. The advantage of this manufacturing strategy was that two C-shaped test specimens could be obtained per braiding and infiltration process by splitting the quadrangular braid. The laminate was therefore cut into two separate specimens with a wet saw after the infusion. In Figure 2 the braiding process and the fixed test specimens within the aluminium fittings are shown. The braiding of a quadrangular shaped form leads to considerable changes of the braiding tow angles. This relation could also be observed in the manufactured test specimens.

The specimens were braided on a radial braiding machine with 176 bobbins and 88 feedings for zero degree in a 2x2 pattern. Toho Tenax® E HTS40 12K F13 carbon fibers, Teijin Twaron® D2200 Aramid fibers and Owens Corning FliteStrand® S ZT glass roving were used as braider yarns. The aerospace qualified resin RTM6 was infused in a VARI process obtaining an averaged fibre volume ratio of 58.1 %. All specimens consisted of 4 braided layers.

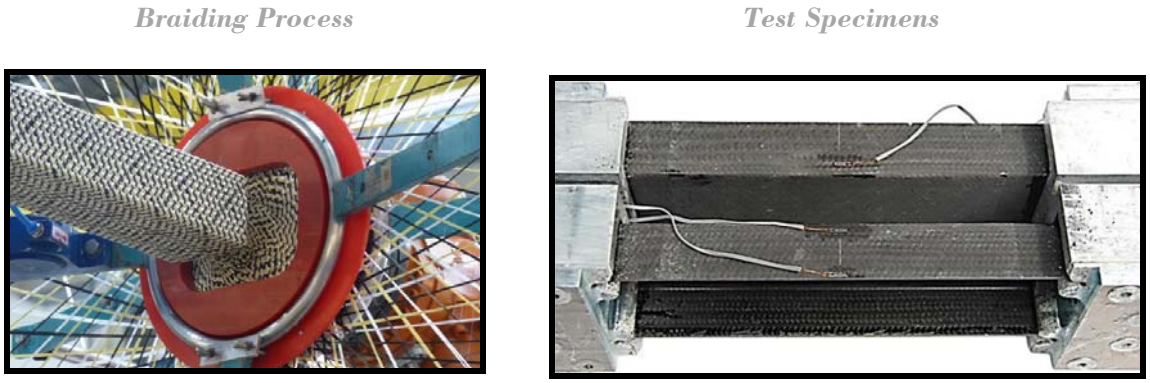

Fig. 2: Braiding process and test specimens embedded in the aluminium clamping

Integration of hybridised axial yarn in the web *(picture type 6)*

Hybridisation of the axial yarn in the flange *(picture type 5)*

Inclusion of a sheet of steel in the web *(picture type 8)*

Hybridisation of the braider tows *(picture type 10)*

Fig. 3: Braided frames with enhanced energy absorption capacity

The main focus of the study conducted was the identification of design strategies for braided frames with improved energy absorptions capacity under bending. Different strategies were investigated for the improvement of the energy absorption. These design strategies were

- modification of the braid angle;
- inclusion of additional standing yarns in the web;
- hybridisation of the standing yarns;
- hybridisation of the bias yarn;
- embedding of a steel sheet in the web for plastification.

Figure 3 shows cross sections of braided frame segments with different hybridization designs. As reference design a carbon frame with 4 layers of biaxial braid in the web and triaxial braid in the flanges was defined *(Braid-Ref-45)*.

Table 1
Material definitions and layup of the test specimen

Nr.	Test Specimen	Description	Flange Laminate	Web Laminate
1	Braid-Ref-45	Reference design [45° braid]	4 x Tri (CF)	4 x Bi (CF)
2	Multi-Ref-45	Frame consisting out of multiaxial fabrics	4 x [45/0/-45] (CF)	4 x [45/0/-45] (CF)
3	Braid-Biax-60	Reference design [60° braid]	4 x Tri (CF)	4 x Bi (CF)
4	Braid-Triax-45	Frame with tri-axial braided web [45°]	4 x Tri (CF)	4 x Tri (CF)
5	Braid-Hyb-GF-FL	Frame with glass-hybridized flange [45°]	4 x Tri (GF<0°>/CF)	4 x Bi (CF)
6	Braid-Hyb-GF-WE	Frame with glass- hybridized web [45°]	4 x Tri (CF)	4 x Tri (GF<0°>/CF)
7	Braid-Hyb-Ara-WE	Frame with Aramid- hybridized web [45°]	4 x Tri (CF)	4 x Tri (Ara<0°>/CF)
8	Braid-Hyb-Met-WE	Frame with steel- hybridized web [45°]	4 x Tri (CF)	4 x Bi (CF) / Steel 1mm
9	Braid-Hyb-GF-CB	Frame consisting out of glass braid [45°]	4 x Tri (CF<0°>/GF)	4 x Bi (GF)
10	Braid-Hyb-ACG-CB	Frame consisting out of hybridized braid [45°]	4 x Tri (CF<0°>/<GF,AF,CF>)	4 x Bi (<GF,AF,CF>)

Bi : biaxial braid *CF : carbon fiber [Toho Tenax® E HTS40 12K]* *GF : glass fiber [Owens Corning FliteStrand® S ZT]*
Tri : triaxial braid *AF : aramid fiber [Teijin Twaron® D2200]*

The finale test matrix included 9 different frame concepts. A short description of all investigated concepts with the layup of flange and web is given in Table 1. Two specimens were built and tested separately for each frame concept for verification of the obtained test results.
Additionally to the braided specimens the frame concept *(Multi-Ref-45)* was defined consisting of multi-axial non-crimped fabric with Tenax HTS40 F13 12K fibres. In this concept each braid direction of frame concept 4 *(Braid-Triax-45)* was replaced by one layer of non-crimped fabric to identify the difference in the material behaviour between braided and conventional frame designs consisting of non-crimped fabric composite material.

3. Test Procedure

The quasi-static tests were performed in a Zwick Roell 1475 universal testing machine with a constant crosshead velocity of v_{St} = 4 mm/min and a maximum crosshead displacement of s = 30 mm, which is far beyond failure initiation. Considering the rotational displacement of the rigid aluminium casings the final displacement corresponds to a final test angle of approximately 20°. A 100 kN load cell, positioned directly above the indenter, was used for force measurement. The displacement, corrected by the stiffness characteristics of the machine and test setup, was obtained directly from the crosshead.
All conducted bending tests showed the typical failure behavior of composite structures. Shortly before failure the compressed flange buckled, initiating a failure in the upper radius. The crack propagated through the compressive loaded flange into the web. For braided specimens with biaxial fiber architecture in the web, the crack propagated along the bias tow angle to the tensile loaded flange. All specimens showed a very abrupt failure initiation with little pronounced nonlinearity in the force-deflection curve, as is typical of fiber dominated failure of carbon/epoxy materials.
In Figure 4 pre- and post-failure pictures of the braided reference frame *(Braid-Ref-45)* and the frame made out of non-crimped fabric *(Multi-Ref-45)* are shown. A significant difference was obtained in the interlaminar failure behavior. The reduced delamination length obtained for the braided frames can be explained by the interlocking nature of braided composite.

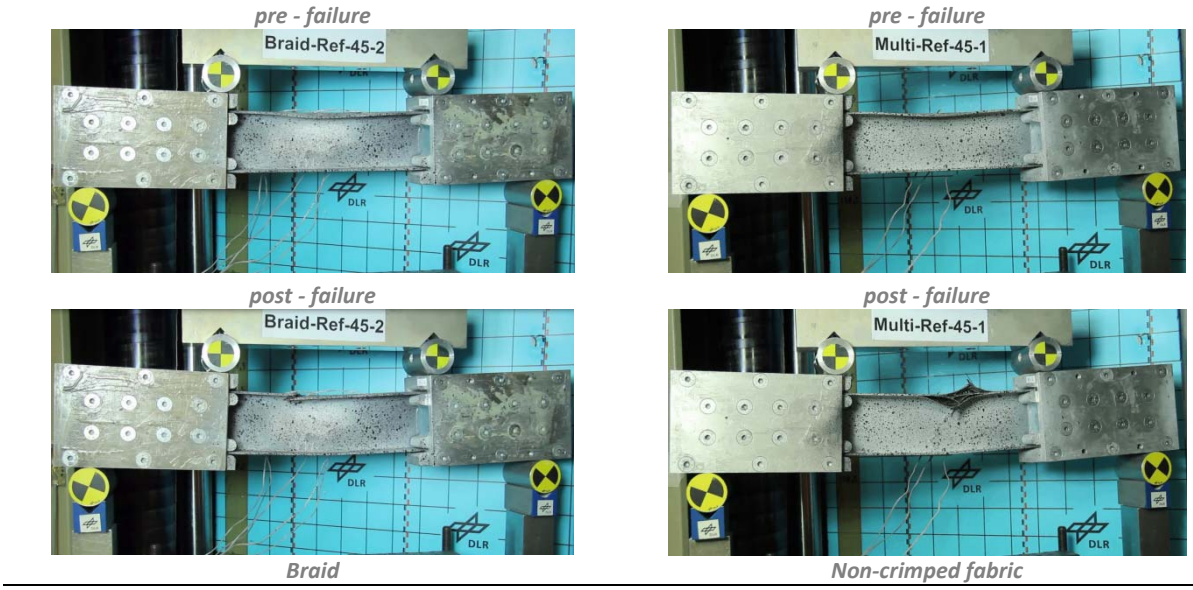

Fig. 4: Pre- and post-failure pictures of frames under four-point-bending

4. Failure modes

For detailed understanding of the failure modes 3D CT-Scans of tested specimens were conducted. Images of flange and web damage are provided for the frame concepts 1 to 4 in Figure 5. The CT-Scan of braided frame *(Braid-Ref-45*) underlines the localized fracture mode already visible in the test.

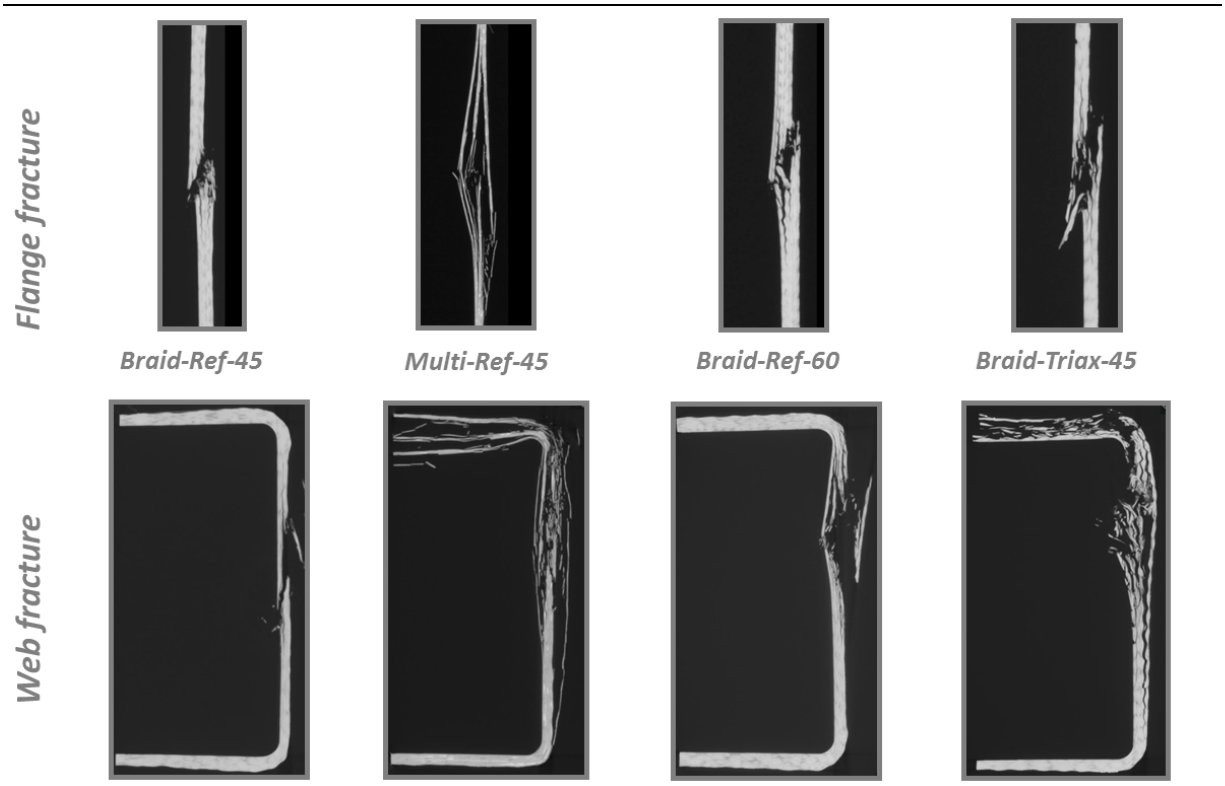

Fig. 5: Visualisation of different fracture modes using 3D CT-Scans

Web and flange show limited interlaminar damage for the reference frame *(Braid-Ref-45)*. Similar failure is obtained for the frame concept with a braiding angle of 60° *(Braid-Ref-60)*. The failure characteristic is affected by the added additional CFRP standing yarns in the web *(Braid-Triax-45)* leading to larger interlaminar damage. The frame made out of non-crimped fabrics disintegrated completely in the fracture zone of web and frame during bending failure. The more localized fracture modes of the braided frames support the assumption that the tow waviness of braids acts as reinforcement through thickness providing an improved damage tolerance for those structures.

The experiments also showed that the fracture behaviour of braided composites can be influenced by the modification of the fibre architecture. Residual structural integrity of the web after failure is essential, if further energy were absorbed in the post-failure domain. Therefore different strategies were investigated with the main objective to prevent crack propagation through the frame web after bending failure. In this context the integration of standing yarns into the web, the hybridisation of the bias yarn and the embedding of a metal sheet in the web were investigated. The observed web failure modes are provided in Figure 6. The failure of the conventional frame design shows the typical fracture characteristics of frames under bending having biaxial braid architecture in the web. The crack propagates through the web along the bias tows. The results show, that this failure behaviour can be influenced by all investigated web modifications. The inclusion of additional standing yarns in the web prevents the failure path along the braid angle. Especially if a tough fibre such as Aramid is used as standing yarn, the integrity of the frame web can be retained up to large bending angles.

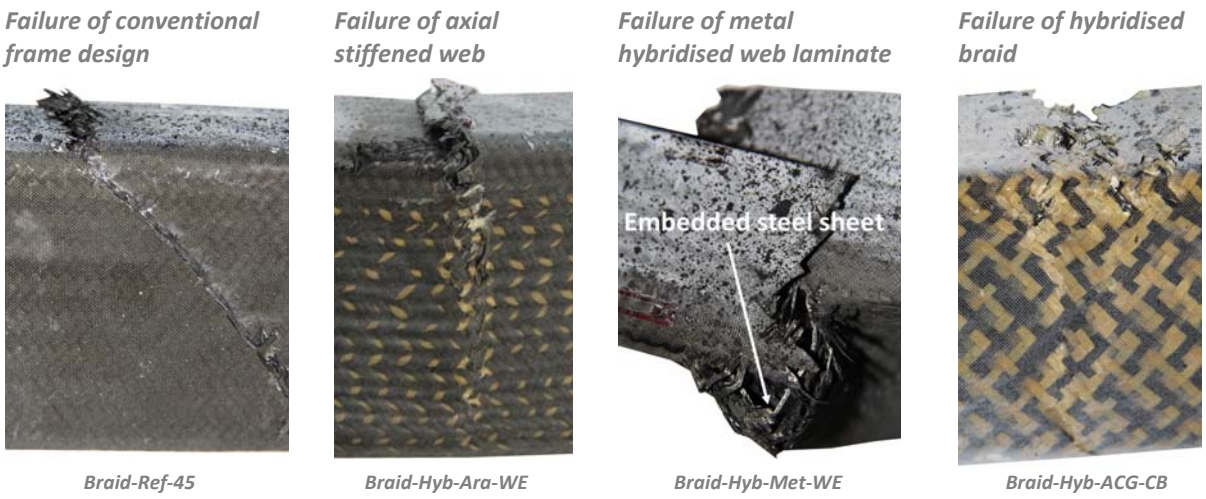

Fig. 6: Failure of the different frame concepts

Thus standing yarns in the web act as crack stoppers, which is important to enable energy absorption in the post-failure domain. The same crack stopping function can also be obtained by hybridisation of the braider tows, since the facture path along the braider tows is influenced by the different material properties of the integrated tougher braider tows. The frame with the embedding metal sheet shows a typical metal failure of the web. The metal sheet successfully prevents the complete rupture through the web, shifting the typical composite fracture to a buckling behaviour. However, the composite plies delaminated from the metal sheet within the fracture zone indicating a weak bonding. The debonding of the metal sheet limited the energy absorption capacity in the post-failure domain since plastification is restricted to the area of the buckles.

5. Results and Discussions

5.1. Summary of the test results

In general, two specimens were tested separately for each frame design to validate and to average the two test responses. The second test result of frame concept 8 (Braid-Hyb-Met-WE) could not be used for evaluation due to a frame failure close to an aluminum fitting. Figure 7 shows the crosshead force-displacement characteristics for a selected number of frame concepts. The specimens show a pronounced linear behavior with a very distinct drop after failure initiation. The force-plateau in the post failure regime differs for the investigated frames which indicates the different energy absorption capacities of the frame concepts. The low absorption plateau of the reference frame concept *(Braid-Ref-45)* shows, that a modification of the braid architecture is required, if considerable energy has to absorbed after bending failure.
For evaluation of the loading capacity of the corresponding frame concepts the peak load during failure initiation can be used. Table 2 compares the mass specific failure load F_{MAX}, the deflection s_{MAX} at failure and the measured tensile ε_{T_max} and compressive ε_{C_max} strain values, measured with strain gauges in the radius between web and flange (Figure 1). Additionally the deviation between the two test results is given to evaluate the reproducibility of the conducted bending tests. The low deviations in loading, deflection and tensile strain indicate a robust and reproducible failure behavior. The larger discrepancies in the compressive strain ε_{C_max} can be explained by slightly varying buckling modes.

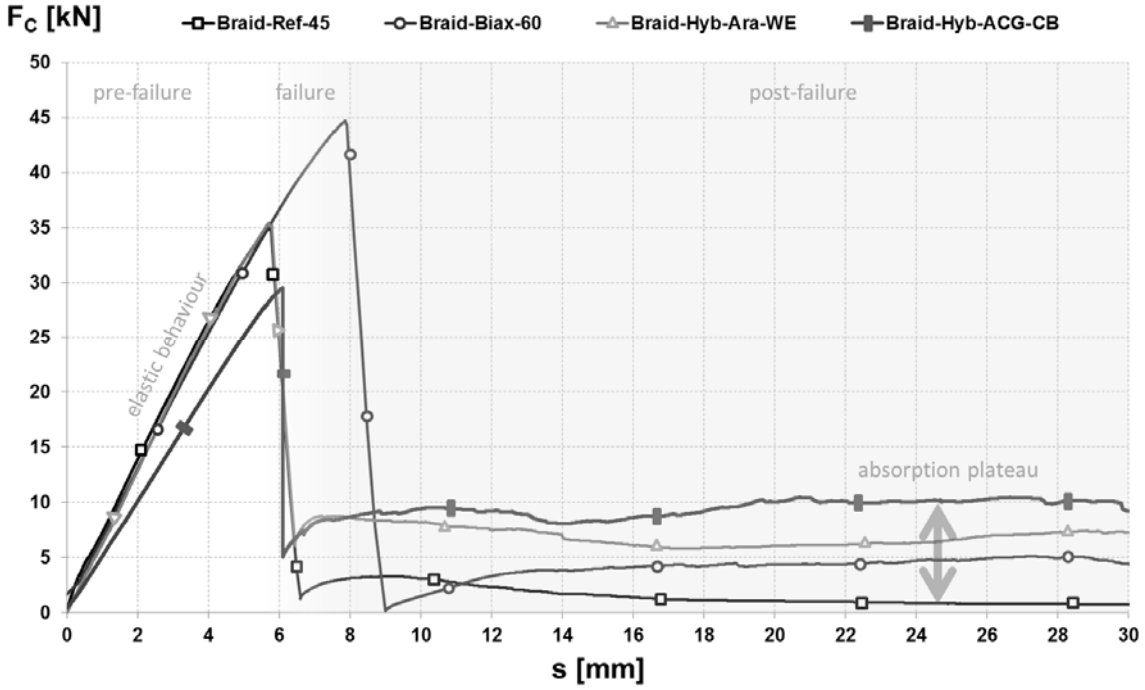

Fig. 7: Crosshead-load deflection curve for four different frame concepts

For comparing the energy absorption capacity in the post-failure domain the averaged mass specific indenter force after 30 mm deflection (~20° bending angle) is also given in Table 2. For some conducted tests significant deviation between two identical tests are obtained indicating a different post-failure behaviour. The difference in the post-failure behaviour mainly depended on the interaction of the two frame segments. Whilst in the most cases the two frame segments were sliding along each other without significant contact forces, in some cases the two frame parts blocked each other leading to composite crushing between the two contact partners. Since this failure behaviour requires two separated frame segments this difference in failure characteristics was only obtained for frames with biaxial fibre architecture in the web.

Table 2
Overview over the test results

Nr.	Test Specimen	m_L[kg/m]	F^*_{MAX} [kN/m_L]		s_{MAX} [mm]		ε_{C_max} [%]		ε_{T_max} [%]		F^*_{30} [kN/m_L]	
1	Braid-Ref-45	0.64	52.08	*3.3 %*	5.72	*0.1 %*	- 8.53	10.9 %	6.78	*2.0 %*	1.07	*8,6 %*
2	Multi-Ref-45	0.69	56.15	*5.2 %*	4.74	*4.6 %*	- 6.82	11.3 %	5.11	*2.1 %*	6.29	*5,1 %*
3	Braid-Biax-60	0.77	59.4	*2.8 %*	8.22	*4.6 %*	- 12.64	1.3 %	9.61	*0.6 %*	8.65	*31,5 %*
4	Braid-Triax-45	0.71	59.59	*0.6 %*	6.37	*2.1 %*	- 7.72	3.4 %	7.19	*0.4 %*	6.44	*0,3 %*
5	Braid-Hyb-GF-FL	0.66	45.71	*2 %*	7.83	*4.6 %*	- 9.88	16.8 %	10.09	*7.8 %*	7.06	*16,6 %*
6	Braid-Hyb-GF-WE	0.76	53.28	*0.1 %*	6.56	*0.7 %*	- 6.24	14.3 %	7.58	*1.9 %*	1.85	*6,1 %*
7	Braid-Hyb-Ara-WE	0.76	45.1	*0.5 %*	5.64	*1.1 %*	- 7.38	12.9 %	5.46	*4.2 %*	9.78	*5,4 %*
8	Braid-Hyb-Met-WE	1.14	37.8	-	5.68	-	- 6.23	-	7.16	-	2.59	-
9	Braid-Hyb-GF-CB	0.90	38.92	*1 %*	7.36	*0.7 %*	- 10.7	14.0 %	7.51	*3.5 %*	8.04	*41,8 %*
10	Braid-Hyb-ACG-CB	0.74	41.38	*3.9 %*	6.69	*6.18 %*	- 7.28	11.4 %	6.59	*4.28 %*	12.39	*8 %*

s_{MAX} : *crosshead displacement at failure*
F^*_{MAX} : *mass specific crosshead force at failure*
F^*_{30} : *mass specific crosshead force at 30 mm displacement*
ε_{C_max} : *compressive failure strain at central flange radius*
ε_{T_max} : *tensile failure strain at central flange radius*
m_L : *mass per specimen length*

Since the structural weight plays a significant role for the airframe design, the weight penalty for improved crashworthiness should be as small as possible. Therefore the weight per unit length was assessed by dividing the mass by the length of the test specimen. The comparison of the values shows that the weight penalty differs significantly for the investigated frame concepts.

5.2. Elastic behaviour

As the braid architecture is changed by adding or replacing fibres from the reference concept, the modification also affects the structural behaviour within the elastic domain. Since stiffness and failure load are important design parameters for the static design process of frames, the influence on the failure load was addressed. The maximum bending moment of the frame segment in a four-point-bending test is calculated by

$$M_{MAX} = \frac{F_{MAX}}{2} L_{\Delta S} \tag{1}$$

where $L_{\Delta S}$ is distance between stamp and support (Figure 1). For approximation of the hinge stiffness, the rotation angle due to the moment load has to be assessed. Considering the rotational displacement of the rigid aluminium casings the angle can be approximated to

$$\gamma = 2\arctan\left(\frac{s}{L_{\Delta S}}\right) \tag{2}$$

were *s* is the displacement of the crosshead. With the change in the bending moment in relation to the change in the rotation angle, the hinge stiffness can be approximated by

$$H = \left(\frac{\Delta M}{\Delta \gamma}\right) \tag{3}$$

Within the study the hinge stiffness was calculated between 1° and 2° rotation angle. For comparison of the elastic bending properties the averaged hinge stiffness and the failure moment are summarized in Figure 8. In Figure 8 the elastic properties are divided by the mass per unit length to make the results mass-specific. The results show, that the static behavior is influenced by the applied modifications. Comparing frame concept 1 *(Braid-Ref-45)* with concept 3 *(Braid-Biax-60)* a significant influence of the braiding angle can be seen.

The comparison shows a small influence of the braiding angle on the bending stiffness which can be explained by the constant numbers of the load carrying axial yarns (0°) in the two concepts (Figure 7). Despite similar stiffness behavior the concept 1 *(Braid-Ref-45)* has a better mass specific elastic behavior, since larger braiding angles are linked with an increase in structural weight. Whilst the results indicate that the mass specific bending stiffness is reduced by the larger braid angle, the modification has a positive influence on the mass specific failure moment M_{MAX}. A postponed buckling initiation of the compressed flange can be assessed for the braiding concept with the increased braid angle *(Braid-Biax-60)*. Two reasons could explain this different behavior. Firstly, the instability of the flange is affected by the increase of the flange thickness from 3.3 mm (45° braid angle) to 4 mm (60° braid angle). Furthermore, the increased stiffness in the transverse direction for the frame concept with 60° braid angle can be assumed to have raised the critical buckling stress. In the literature analytical solutions can be found for the assessment of the buckling behavior of orthotropic plates under various loading conditions [17] [18]. The analytical description of buckling behavior of orthotropic plates shows a direct dependence of the critical buckling stress on the transverse stiffness. For braided frames the transverse stiffness can be increased using a larger braid angle. Since the results indicate that the braiding angle has a strong impact on the maximum failure load, larger braiding angles than 45° are recommended for open frames structures loaded under bending loads.

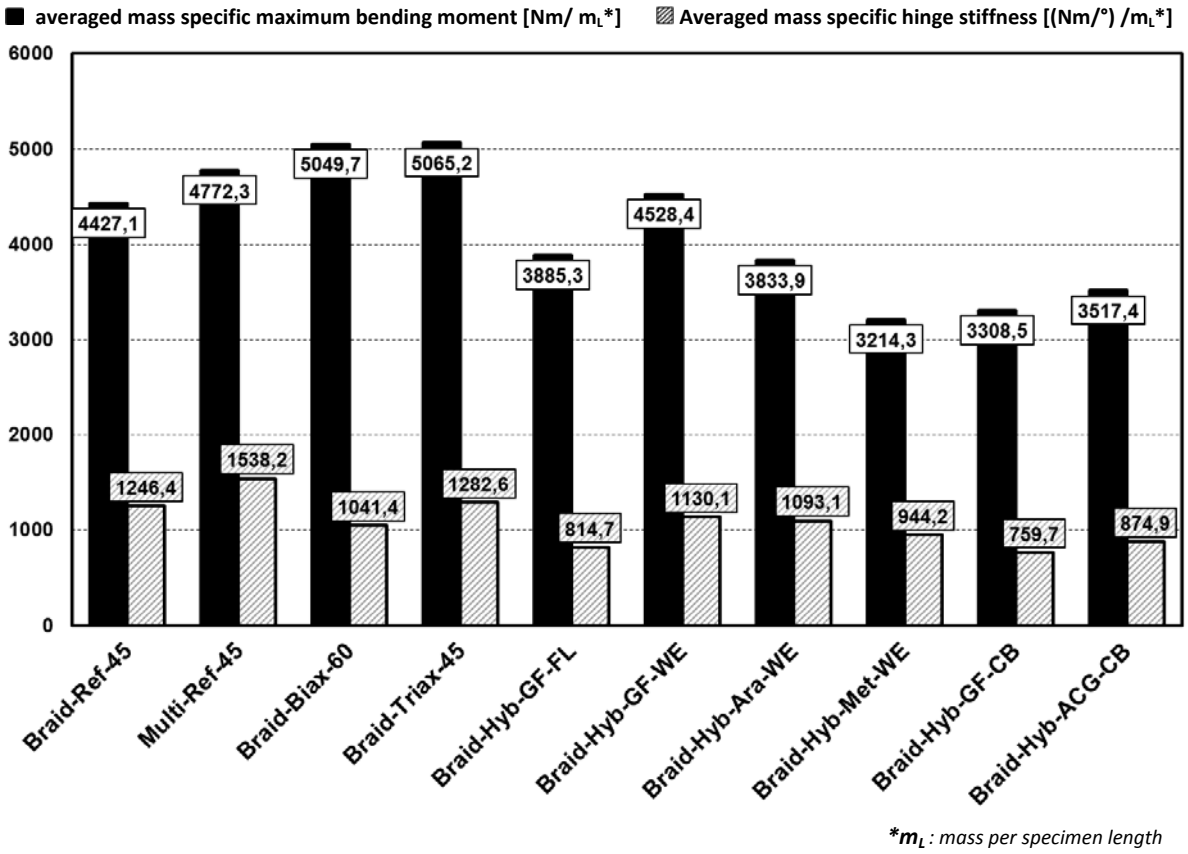

Fig. 8: Overview of the mass specific elastic properties of the investigated frame concepts

The application of additional standing yarns in the frame web *(Braid-Hyb-Ara-WE / Braid-Triax-45 / Braid-Hyb-GF-WE*) increases stiffness and failure moments. Therefore the additional axial fibres in the web could be included in the static design process and could slightly lower the static requirements on the flanges. However, the weight penalty directly depends on the fibre properties of the yarn used.

Hybridisation of braider tows *(Braid-Hyb-GF-CB / Braid-Hyb-ACG-CB)* reduces the elastic stiffness due to the lower elastic performance of glass and aramid in comparison to carbon fibres. The failure moment is also affected by the hybridisation. Considering the change in the elastic behaviour a hybridisation of the braider tows rather negatively affects the structural behaviour within the elastic domain.

As expected a significant reduction of stiffness is obtained by replacing the carbon standing yarns with glass fibres *(Braid-Hyb-GF-FL)*. Since the elastic deformation capability of the glass fibres cannot be exploited due to the initiation of buckling, fibres with pronounced elasticity in the flanges do not seem to be a reasonable strategy to enhance the energy absorption capacity under bending.

The integration of a steel inlay leads to stiffer behaviour and postponed failure initiation. Therefore the steel inlay could also be considered in the static design process. However, the concept shows a low mass specific elastic performance due to the significant weight penalty of 78 %. The weight problem may be reduced using other metals with lower density. However, the difference in the thermal expansion coefficients and the composite-metal interface remain as problems to be considered.

As expected the frame made out of non-crimped fabric *(Multi-Ref-45)* has the largest mass specific hinge stiffness. A direct comparison of this frame with the braided frame *(Braid-Triax-45)* is not possible, since the braided frame included about 6% less fibres in the axial direction. Interestingly the

braided frame could sustain higher bending loads despite the lower hinge stiffness and the same buckling pattern.

5.3. Energy absorption capacity

The scope of the study was the identification of design principles for braided frames with enhanced energy absorption capacity. For estimating of the absorption capability the loading curve of the crosshead was integrated

$$E_{abs} \approx \int F(s)ds \approx \sum_{k=1}^{n} F(s_K)\Delta s \qquad (4)$$

The energy absorption capacity for the investigated frame concept is summarized in Figure 9. For better understanding of the different absorption regimes the energy absorption is additionally separated in the elastic- and post-failure domain. All energy absorptions are divided by the mass per unit length (table 2) to make the results mass-specific.
The outcomes indicate that the often recommended design for frames with shear optimized web (+/- 45° fibre direction) shows limited energy absorption capability. Particularly the energy absorption in the post-failure domain after the crack propagated along the bias yarn directly through the web limits the energy absorption in the post-failure domain of frames having biaxial fibre architecture in the web *(Braid-Ref-45)*.

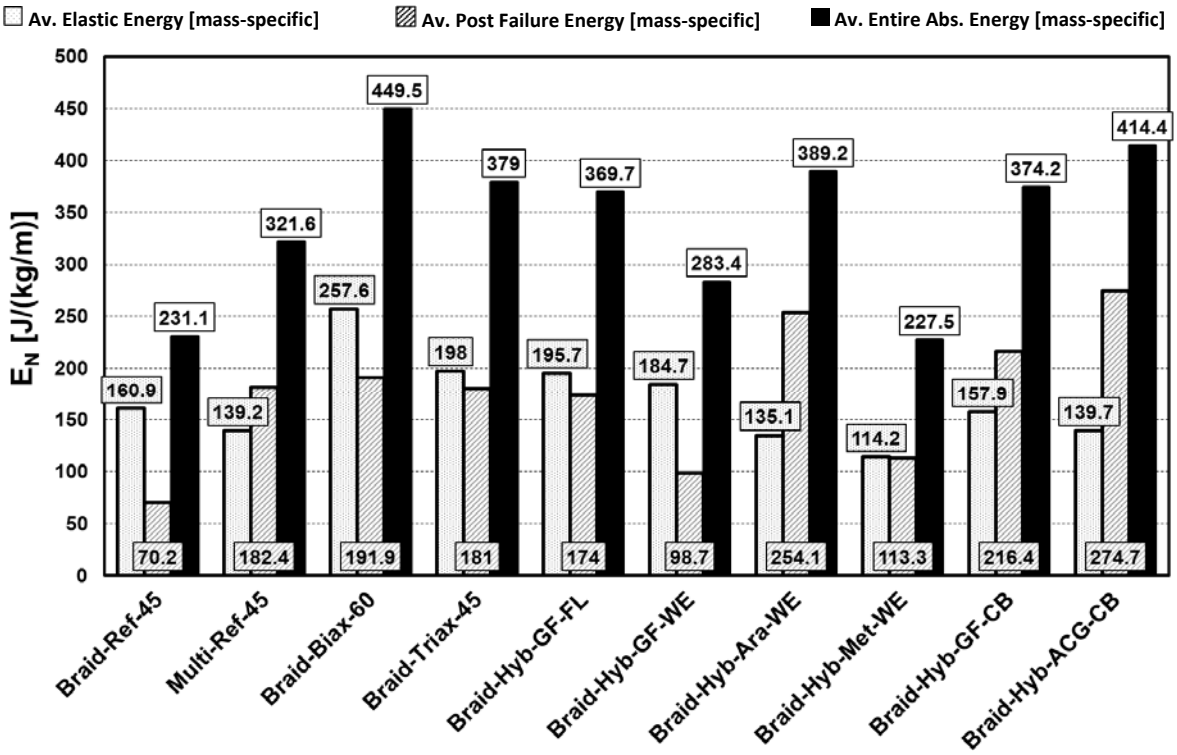

Fig. 9: Overview of the energy absorption capacity of the investigated frame concepts

The comparison of the frame concepts made out of non-crimped fabrics *(Multi-Ref-45)* and the corresponding braided frame *(Braid-Triax-45)* shows similar energy absorption capacity in the post-failure domain. This indicates that the braided fibre architecture alone does not considerable increase the energy absorption capacity in the post-failure domain. A local modification of the fibre architecture is required for braided frames with enhanced post-failure energy absorption.

The change of the braid angle from 45° *(Braid-Ref-45)* to 60° *(Braid-Ref-60)* significantly increases the mass specific energy absorption. The increase in the elastic regime can be explained by the postponed buckling of the compressed flange as described above. The energy absorption in the post-failure domain also increases. However, it should be mentioned, that in one test the two contact segments blocked each other after failure leading to local crushing of the two frame segments with increased energy absorption.
The integration of standing yarns in the web proved to be an efficient technique to enhance the energy absorption capacity after bending failure. By integration of tough fibres such as aramid *(Braid-Hyb-Ara-WE)* the energy absorption in the post failure domain can be increased, whilst the use of stiffer fibres such as carbon fibres *(Braid-Triax-45)* increases the maximum elastic stored energy before failure. The application of glass fibres as standing yarn in the web *(Braid-Hyb-GF-WE)* seems not recommendable.
The comparable low energy absorption capacity of the frame concept with metal inlay *(Braid-Hyb-Met-WE)* can be explained by the debonding of the metal inlay from the braided layers during failure, leading to low energy absorption in the post-failure domain. Due to the failure of the interface plastification was only obtained in the area of the folds. The high density of the metal inlay reduces further the mass specific energy absorption.
The results further indicate that hybridisation of the braiding tows is also an efficient way to improve the energy absorption in the post-failure domain *(Braid-Hyb-GF-CB / Braid-Hyb-ACG-CB)*. However, in contrast to the integration of standing yarn in the web, the hinge stiffness can be reduced if the used fibres have lower elastic properties compared to the original carbon fibres. Therefore, the replacement of the carbon fibres led to a reduced static performance.

6. Conclusions

The bending failure of C-shaped braided frame segments was investigated under four-point-bending loads. Low energy absorption in the post-failure domain was found for standard braided frames with biaxial fibre architecture in web. The experiments showed that the fracture behaviour of braided composites can be influenced significantly by the modification of the fibre architecture in the web. Residual structural integrity of the web after failure is essential, when further energy absorption is required in the post-failure domain. Thus different strategies were investigated with the main objective to prevent instantaneous crack propagation through the frame web after bending failure. By integration of additional standing yarns in the web the failure characteristics of the frame can be influenced. While the use of stiffer fibers such as carbon fibres increases the maximum elastic stored energy before failure, the energy absorptions in the post-failure domain can be increased by the application of tough fibres in the web. By hybridisation of the braider tows the energy absorption in the post-failure domain can be increased, however, the modification reduces the elastic properties of the frame. Comparably low energy absorption capacity was obtained for the frame concept with metal inlay in the web. Due to the debonding of the metal sheet during failure plastification was restricted to the area of local folds.
Since the results show a direct dependency of the critical buckling stress from the transversal stiffness of the compressed flange, larger braiding angles than 45° are recommended for open frames structures under bending load.
Currently the studies were conducted under quasi-static loading conditions. Future work should investigate the rate dependency of the observed energy absorption concepts. Further studies should address the application of the design principles on closed frames such as Omega shaped frames in combination with a part of the skin.

Acknowledgements

The research leading to these results has partially received funding from the Helmholtz Association of German Research Centres. The authors gratefully acknowledge the funding of the research activities. The first author also thanks R. Landsberger for his support in the test activities.

References

[1] P. Falzon, I. Herszberg, *Mechanical performance of 2-D braided carbon/epoxy composites,* Composites Science and Technology, Volume 58, Issue 2, 1998

[2] S. Swanson, L. Smith, *Comparison of biaxial strength properties of braided and laminated carbon fiber composites,* Composites: Part B, Volume 27B, 1996

[3] L. Smith, S. Swanson*, Strength design with triaxial braid textile composites,* Composites science and Technology, Volume 56, 1996

[4] P. Potluri, A. Manan, M. Francke, R. Day, *Flexural and torsional behaviour of biaxial and triaxial braided composite structures*, Composite Structures, Volume 75, 2006

[5] R. Böhm, A. Hornig, J. Luft et al., *Experimental Investigation of the Strain Rate Dependent Behaviour of 2D Biaxially and Triaxially Reinforced Braided Composites,* Applied Composites Material, Volume 21, 2014

[6] P. Potluri, A. Manan, *Mechanics of non-orthogonally interlaced textile composites*, Composites: Part A, Volume 38, 2007

[7] K. Birkefeld, M. Röder, T. Reden et al., *Characterization of Biaxial and Triaxial Braids: Fiber Architecture and Mechanical Properties,* Applied Composites Material, Volume 19, 2012

[8] J. Schultz, M. Garnich, *Meso-scale and multicontinuum modelling of a triaxial braided textile composite,* Journal of Composite materials, 2012

[9] X. Li, W. Binienda, R. Goldberg, F*inite element model for failure study of two-dimensional triaxially braided composite*, NASA/TM-2010-216372, 2010

[10] M. Fouinneteau, *Damage and failure modelling of carbon and glass 2D braided composites, PhD thesis*, Cranfield University, 2006

[11] M. Waimer, *Development of a Kinematics Model for Assessment of Global Crash Scenarios of a Composite Transport Aircraft Fuselage,* PhD thesis, University of Stuttgart, ISRN DLR-FB-2013-28, 2013

[12] P. Schatrow, M. Waimer, *Investigation of a crash concept for CFRP transport aircraft based on tension absorption,* International Journal of Crashworthiness, Volume 19, Issue 5, 2014,

[13] R. Sturm, Y. Klett, C. Kindervater, H. Voggenreiter, *Failure of CFRP airframe sandwich panels under crash-relevant loading conditions,* Journal of Composite Structures, Vol. 112, pp. 11-21, 2014

[14] J. Pérez, *Energy Absorption and Progressive Failure Response of Composite Fuselage Frames*, Master thesis, Virginia Polytechnic Institute, 1999

[15] S. Heimbs, M. Hoffmann, M. Waimer et al., *Dynamic Testing and Modelling of Composite Fuselage Frames and Fasteners for Aircraft Crash Simulations*, International Journal of Crashworthiness, Vol. 18, No. 4, 2013, pp. 406-422

[16] M. Waimer, D. Kohlgrüber, R. Keck, H. Voggenreiter, *Contribution to an improved crash design for a composite transport aircraft fuselage - development of a kinematics model and an experimental component test setup*, CEAS Aeronautical Journal, Volume 3, 2013

[17] P. M. Weaver, M. Nemeth, *Improved Design Formulas for Buckling of Orthotropic Plates Under Combined Loading*, AIAA Journal, Vol. 46, No. 9 (2008), pp. 2391-2396.

[18] I. Hwang, J. Lee, *Buckling of orthotropic plates under various inplane loads*, KSCE Journal of Civil Engineering, Volume 10, 2006

Keywords: Braids, bending failure, hybridisation, energy absorption, crash